Increased Persistent Sodium Current Causes Neuronal Hyperexcitability in the Entorhinal Cortex of *Fmr1* Knockout mice

Pan-Yue Deng and Vitaly A. Klyachko

SUPPLEMENTAL INFORMATION:

Supplemental Figures:

Figure S1 (Related to Figure 1). Intrinsic membrane properties are unaltered in EC layer III PCs of *Fmr1* KO mice.

Figure S2. (Related to Figure 2). Changes in tonic excitatory/inhibitory inputs do not account for the increased excitability of EC layer III PCs in *Fmr1* KO mice

Figure S3. (Related to Figure 4). Combined inhibition of NMDA, AMPA, $GABA_A$ and $GABA_B$ receptors does not affect differences in I_{NaP} between *Fmr1* KO and WT EC layer III PCs.

Supplemental Experimental Procedures

Supplemental References

SUPPLEMENTAL FIGURES

FUGURE S1

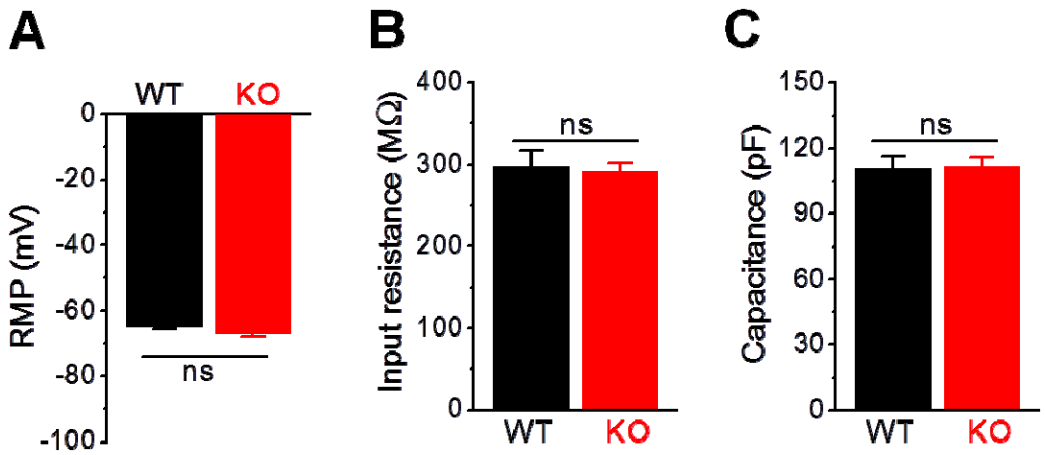

Figure S1 (Related to Figure 1). Intrinsic Membrane Properties are Unaltered in EC Layer III PCs of *Fmr1* KO Mice.

(**A,B,C**) No detectable changes in resting membrane potential (RMP) (**A**), input resistance (**B**) and cell capacitance (**C**) in EC layer III pyramidal cells of *Fmr1* KO mice. RMP: WT n = 55; KO n = 66, p = 0.148; Input resistance: WT n = 6; KO n = 6, p = 0.764; Capacitance: WT n = 55; KO n = 66, p = 0.803, ns, not significant.

FIGURE S2

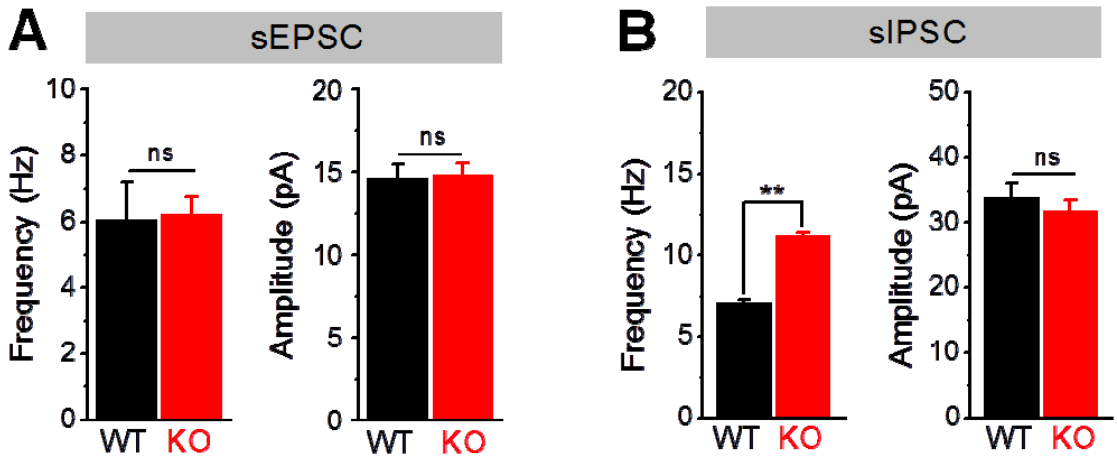

Figure S2 (Related to Figure 2). Changes in Tonic Excitatory/Inhibitory Inputs Do Not Account for the Increased Excitability of EC Layer III PCs in *Fmr1* KO Mice

(**A, B**) Frequency and amplitude of sEPSC (**A**) (WT n = 6, KO n = 6; frequency: p = 0.519; amplitude: p = 0.690) or sIPSC (**B**), (WT n = 6, KO n = 6; sIPSC frequency: p = 0.0071; sIPSC amplitude: p = 0.449) recorded in layer III pyramidal cells of *Fmr1* KO and WT mice.

** $p < 0.01$, ns, not significant.

We note that elevated sIPSC frequency cannot account for increased PC excitability unless the GABAergic transmission has an excitatory action in *Fmr1* KO neurons (He et al., 2014). However, this is unlikely to be the case in our recordings that were performed at P20-25, well beyond the developmental point of the $GABA_A$ receptor polarity switch in *Fmr1* KO mice (He et al., 2014). Moreover, we estimated the $GABA_A$ receptor reversal potential to be -59 mV for both genotypes in our recordings, which implies inhibitory action of GABA near the threshold potentials in both genotypes. Furthermore, we found that inhibition of GABAergic transmission failed to affect the difference in threshold between genotypes (**Figure 4A**). Therefore, a likely explanation is that elevated tonic GABAergic transmission in *Fmr1* KO mice is a compensatory effect against increased excitability in the EC network of FXS mice.

FIGURE S3

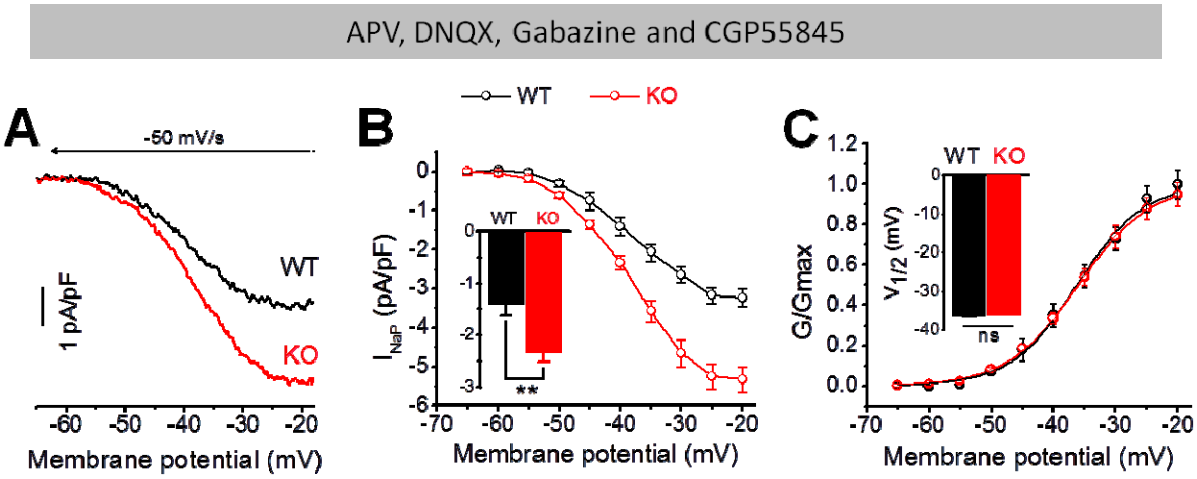

Figure S3. (Related to Figure 4). Combined inhibition of NMDA, AMPA, $GABA_A$ and $GABA_B$ receptors does not affect differences in I_{NaP} between *Fmr1* KO and WT EC layer III PCs.

Sample I_{NaP} traces (**A**) and summarized data (**B**, Insert, I_{NaP} at -40 mV) for I_{NaP} measured in the presence of 4 blockers (against NMDA, AMPA, GABAA and GABAB receptors). The voltage-dependent activation of I_{NaP} in *Fmr1* KO neurons was not affected in the presence of these 4 blockers (**C**, Insert, $V_{1/2}$ of I_{NaP} activation). ** $p < 0.01$; ns, not significant.

SUPPLEMENTAL EXPERIMENTAL PROCEDURES

Animals and slice preparation

Fmr1 KO and WT control mice on FVB background were obtained from The Jackson Laboratory. Slices were prepared as previously described (Deng et al., 2013). In brief, both male and female 20–25-day-old mice were used. After being deeply anesthetized with CO_2, mice were decapitated and their brains were dissected out in ice-cold saline containing the following (in mm): 130 NaCl, 24 $NaHCO_3$, 3.5 KCl, 1.25 NaH_2PO_4, 0.5 $CaCl_2$, 5.0 $MgCl_2$, and 10 glucose, pH 7.4 (saturated with 95% O_2 and 5% CO_2). Horizontal brain slices (350 μm) including the entorhinal cortices were cut using a vibrating microtome (Leica VT1100S). Slices were initially incubated in the above solution at 35°C for 1 h for recovery and then kept at room temperature (~23°C) until use. All animal procedures were in compliance with the US National Institutes of Health Guide for the Care and Use of Laboratory Animals, and conformed to Washington University Animal Studies Committee guidelines.

Action potential recording and threshold determination

Whole-cell patch-clamp recordings using a Multiclamp 700B amplifier (Molecular Devices) in current-clamp mode were made from pyramidal or stellate cells of EC superficial layers visually identified with differential interference contrast optics (Olympus BX51WI). Current-clamp recordings were made with pipette capacitance compensation and bridge-balance compensation. Pyramidal and stellate cells were identified according to the morphology and electrophysiological properties, as previously described (Deng et al., 2007). All of the recordings were conducted at near-physiological temperature (33–34°C). The recording electrodes were filled with the following (in mM): 130 K-gluconate, 10 KCl, 0.1 EGTA, 2 $MgCl_2$, 2 ATP_2Na, 0.4 GTPNa, and 10 HEPES, pH 7.3. The extracellular solution contained (in mM): 125 NaCl, 24 $NaHCO_3$, 3.5 KCl, 1.25 NaH_2PO_4, 2 $CaCl_2$, 1 $MgCl_2$, and 10 glucose, pH 7.4 (saturated with 95% O_2 and 5% CO_2). APs were evoked by a ramp current injection (0.1-0.15 pA/ms) (Yamada-Hanff and Bean, 2013) with a hyperpolarizing onset to ensure maximal Na^+ channel availability before the 1st AP. The AP thresholds were determined from the first APs of ramp-evoked AP trains, unless otherwise stated. For spontaneous AP recordings, the RMP was set to ~ -51 mV via automatic slow current injection. AP threshold (i.e., threshold voltage) was defined as the voltage at the AP turning point, corresponding to the first peak of 3rd order derivative of AP trace (Lu et al., 2012). Ramp current-evoked AP threshold was defined as the mean threshold

of the first AP averaged over 5-8 trials. For spontaneous firing, the AP threshold value for each cell was the mean threshold averaged over APs in a 20 s window.

Persistent Na^+ current recordings

We first used a depolarizing voltage ramp (-100 to -20 mV, 20 mV/s) to evoke I_{NaP} from EC layer III PCs (Figures 3A-C), using the same internal and external solutions as those in AP recording. Under this condition, AP currents that escaped voltage clamp control were present in most of the cells. In order to eliminate the uncontrolled AP currents, we then used a repolarizing ramp (depolarized to +30 for 200ms then ramped back to -65 mV with -50 mV/s) (Figures 3D,E, 4C-H) to record I_{NaP}, using Cs-based internal solution containing 10 mM TEA and 2 mM 4-AP, and replacing 20 mM NaCl with equimolar TEA-Cl and adding 100 μM $CdCl_2$ to normal extracellular solution to minimize K^+ and Ca^{2+} currents. Cell capacitance was compensated. Series resistance compensation was enabled with 80–90% correction and 16 μs lag. I_{NaP} was isolated by subtracting current in 1 μM TTX from that before TTX.

Determination of resting membrane potential, capacitance and input resistance

RMP was measured immediately after whole-cell formation. Cell capacitance was determined by the amplifier's auto whole-cell compensation function with slight manual adjustment to optimize the measurement if needed. The obtained values then were used for whole-cell current normalization. Under current-clamp mode, a negative current (−50 pA for 500 ms) was injected every 5 s to assess the input resistance.

Recordings of sEPSC and sIPSC

The sEPSC was recorded from EC layer III PC with recording electrodes filled with the same internal solution as that of AP recordings. For sIPSC recording, high chloride electrode solution was used (using CsCl to replace K-gluconate and KCl). A total of 5 min of trace was analyzed to estimate sEPSC or sIPSC frequency and amplitude in MiniAnalysis for each cell.

Statistical analysis

Data are presented as mean ± SEM. Student's paired or unpaired t test was used for statistical analysis as appropriate; significance was set as $p < 0.05$. The n was number of cells tested.

SUPPLEMENTAL REFERENCES:

Deng, P.Y., Poudel, S.K., Rojanathammanee, L., Porter, J.E., and Lei, S. (2007). Serotonin inhibits neuronal excitability by activating two-pore domain k+ channels in the entorhinal cortex. Mol Pharmacol *72*, 208-218.

Deng, P.Y., Rotman, Z., Blundon, J.A., Cho, Y., Cui, J., Cavalli, V., Zakharenko, S.S., and Klyachko, V.A. (2013). FMRP regulates neurotransmitter release and synaptic information transmission by modulating action potential duration via BK channels. Neuron *77*, 696-711.

He, Q., Nomura, T., Xu, J., and Contractor, A. (2014). The developmental switch in GABA polarity is delayed in fragile X mice. J Neurosci *34*, 446-450.

Lu, U., Roach, S.M., Song, D., and Berger, T.W. (2012). Nonlinear dynamic modeling of neuron action potential threshold during synaptically driven broadband intracellular activity. IEEE Trans Biomed Eng *59*, 706-716.